Ultrasonic vocalization impairment of Foxp2 (R552H) knockin mice related to speech-language disorder and abnormality of Purkinje cells

Eriko Fujita*, Yuko Tanabe*, Akira Shiota†, Masatsugu Ueda†, Kiyotaka Suwa‡, Mariko Y. Momoi‡, and Takashi Momoi*§

*Divisions of Development and Differentiation, Department of Human Inherited Metabolic Disease, National Institute of Neuroscience, 4-1-1 Ogawahigashi-machi, Kodaira, Tokyo 187-8502, Japan; †YS Institute of Technology, PhoenixBio, Co. Ltd., 1198-4 Iwazo, Utsunomiya, Tochigi 329-0973, Japan; and ‡Department of Pediatrics, Jichi Medical University, 3311-1 Yakushiji, Shimotsukeshi, Tochigi 329-0498, Japan

Communicated by Masao Ito, RIKEN, Wako, Japan, December 28, 2007 (received for review November 16, 2007)

Previous studies have demonstrated that mutation in the forkhead domain of the forkhead box P2 (FOXP2) protein (R553H) causes speech-language disorders. To further analyze FOXP2 function in speech learning, we generated a knockin (KI) mouse for Foxp2 (R552H) [Foxp2 (R552H)-KI], corresponding to the human FOXP2 (R553H) mutation, by homologous recombination. Homozygous Foxp2 (R552H)-KI mice showed reduced weight, immature development of the cerebellum with incompletely folded folia, Purkinje cells with poor dendritic arbors and less synaptophysin immunoreactivity, and achieved crisis stage for survival 3 weeks after birth. At postnatal day 10, these mice also showed severe ultrasonic vocalization (USV) and motor impairment, whereas the heterozygous Foxp2 (R552H)-KI mice exhibited modest impairments. Similar to the wild-type protein, Foxp2 (R552H) localized in the nuclei of the Purkinje cells and the thalamus, striatum, cortex, and hippocampus (CA1) neurons of the homozygous Foxp2 (R552H)-KI mice (postnatal day 10), and some of the neurons showed nuclear aggregates of Foxp2 (R552H). In addition to the immature development of the cerebellum, Foxp2 (R552H) nuclear aggregates may further compromise the function of the Purkinje cells and cerebral neurons of the homozygous mice, resulting in their death. In contrast, heterozygous Foxp2 (R552H)-KI mice, which showed modest impairment of USVs with different USV qualities and which did not exhibit nuclear aggregates, should provide insights into the common molecular mechanisms between the mouse USV and human speech learning and the relationship between the USV and motor neural systems.

KE family | nuclear aggregation | autism | endoplasmic reticulum stress

The phenotype of the speech-language disorder segregates as an autosomal dominant trait. The KE family consists of three generations in which approximately half of the members (15 members) have severe articulation difficulties accompanied by verbal and orofacial impairments. The speech difficulties cannot be fully attributed to the basic impairment of orofacial praxis; the affected KE members normally perform single simple oral movements but have trouble with language comprehension, including grammar as well as production (1–5). Recent studies in the KE family identified the forkhead box P2 (FOXP2) gene as the responsible genetic factor and found that a missense mutation (R553H) in the forkhead domain of FOXP2 cosegregates with the disorder in this family (2–5).

In addition to a forkhead domain with a winged-helix DNA binding domain (6), FOXP2 also contains a glutamine-rich region (polyQ tract), zinc finger, and a leucine zipper motif for homodimerization and heterodimerization with Foxp1, 2, and 4 family members (7). FOXP2 also interacts with the C-terminal binding protein (CtBP) to act as a transcriptional repressor (7). The familial FOXP2 mutated protein (R553H) exhibits reduced DNA binding and defects in nuclear localization *in vitro* (8, 9). In addition, a nonsense mutation (R328X), another mutation related to the speech-language disorder, also confers compromised binding and localization (10). However, despite the extensively studied relationship *in vitro* between the mutation in FOXP2 and pathogenesis of the speech-language disorder, the molecular mechanisms that contribute to the disorder are still unresolved, underscoring the need for an animal model for the analysis of the speech learning and disorder at the molecular level.

FoxP2 function appears to be evolutionary conserved across multiple species; high levels of FoxP2 have been detected during vocal learning in zebra finches (11), and the expression pattern of FoxP2 of songbirds changes during the seasons. The structure of FoxP2 is highly conserved during evolution as well (12), because the human FOXP2 protein differs at only 2 aa compared with its mouse homologue, along with one glutamine from the human protein that is absent in the polyQ tract in mouse Foxp2 (12). Human FOXP2 and mouse Foxp2 show quite similar expression patterns in the developing brain, with expression detected in the cortical plate, basal ganglia, thalamus, and inferior olive (13, 14).

Infant rodents emit ultrasonic vocalizations (USVs), whistle-like sounds with frequencies between 40 kHz and 100 kHz, when isolated from the mother and littermates (15). These signals play an important communicative role in mother–offspring interactions because they elicit prompt responses from the dam concerning caregiving behaviors (15). Homozygous Foxp2-knockout (KO) mice display severe motor impairment, premature death, and an absence of USVs in response to stress (16). Heterozygous Foxp2-KO mice also display modest developmental delays and significant alterations in USVs. Thus, it is likely that Foxp2 plays an essential role in the production of USVs required for the social communication functions of mice. However, it is not clear whether mouse USVs and human speech share a common molecular mechanism regulated by Foxp2.

To clarify the relationship between the FOXP2 (R553H) mutation and the pathogenesis of the speech-language disorders and to examine the Foxp2-mediated common molecular mechanism between mouse USVs and human speech, we generated knockin mice [Foxp2 (R552H)-KI] for the mouse homologue of FOXP2 (R553H) by homologous recombination. Here we show evidence for a common molecular mechanism shared between human speech and mouse USVs and discuss the defect of this molecular mechanism and immature development of cerebellum in the Foxp2 (R552H)-KI mice.

Author contributions: M.Y.M. and T.M. designed research; E.F., Y.T., and T.M. performed research; E.F., A.S., M.U., K.S., and M.Y.M. contributed new reagents/analytic tools; E.F., Y.T., M.Y.M., and T.M. analyzed data; and E.F. and T.M. wrote the paper.

The authors declare no conflict of interest.

§To whom correspondence should be addressed. E-mail: momoi@ncnp.go.jp.

This article contains supporting information online at www.pnas.org/cgi/content/full/0712298105/DC1.

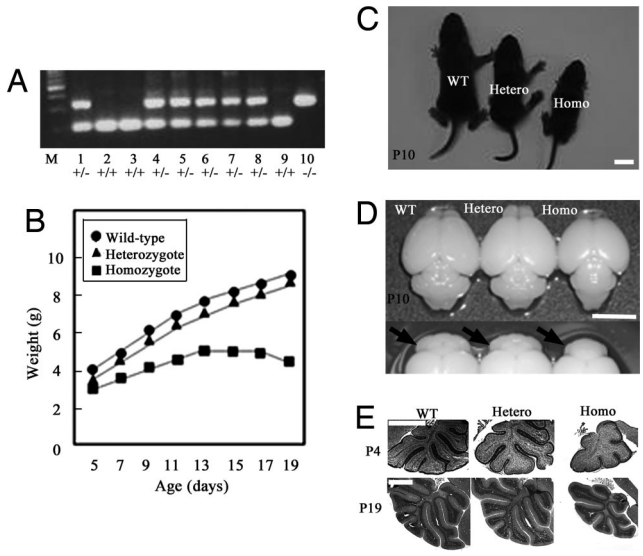

Fig. 1. Characterization of the Foxp2 (R552H)-KI mice. (*A*) Genotype assay by PCR. Lanes 1–10, littermates; lane M, molecular size marker. (*B*) Postnatal weight of pups over time. (*C* and *D*) Pups (*C*) and brains (*D*) of wild-type, heterozygous, and homozygous Foxp2 (R552H)-KI mice (P10). Arrows indicate the cerebella. The size of the homozygous cerebellum is smaller than the wild-type and heterozygous ones. (*E*) Hematoxylin and eosin staining of the cerebella at P4 and P19. Hetero, heterozygote; Homo, homozygote. (Scale bars: *C* and *D*, 5 mm; *E*, 1 mm.)

Results

Characterization of Knockin Mouse with R552H Mutation, Foxp2 (R552H)-KI, and Defect of the Coordinated Movement. We generated mice harboring the mutation in Foxp2 homologous to the mutation in the KE family with the speech-language disorder [Foxp2 (R552H)-KI mice] [supporting information (SI) Fig. 6]. Genotypes of wild-type, heterozygous, and homozygous Foxp2 (R552H)-KI mice were assessed by PCR analysis for the allele retaining a single loxP site (Fig. 1*A*) after blind behavioral analyses. Offspring genotypes from heterozygous matings did not approach Mendelian frequencies (wild-type:heterozygote:homozygote, 69:155:27), suggesting that approximately half of homozygotes are embryonic lethal or die at birth and may be immediately eaten by the mother. Similar to the Foxp2-KO mice, homozygous Foxp2 (R552H)-KI mice did not grow at a normal rate 20 days after birth, although they showed a milk strip (milk materials in the stomach). At postnatal day 10 (P10), a significant difference in mean weight (30–40% reduction) was detected between homozygous Foxp2 (R552H)-KI mice and wild-type littermates and increased over the next 10 days because of the further weight reduction of the homozygous Foxp2 (R552H)-KI mice, whereas a 10–15% difference remained between heterozygous and wild-type mice (Fig. 1*B*). Homozygous Foxp2 (R552H)-KI mice (P10) were ≈30% smaller than heterozygous or wild-type mice (Fig. 1*C*). The brain size, particularly the cerebellum, of the homozygote (P10) was also smaller than that of the heterozygous and wild-type mice (Fig. 1*D*). The development of folia of the homozygous cerebellum (P4–P19) was morphologically immature with less folia that were incompletely folded (Fig. 1*E*). The delay of the morphological development was not observed in most heterozygous cerebella (P19) (Fig. 1*E*).

Motor and USV Impairment in Homozygous and Heterozygous Foxp2 (R552H)-KI Mice. The affected members in the KE family have impairment of coordinated movements that are required for speech (verbal and orofacial dyspraxia) and impairment of speech and verbal comprehension (dysphasia) (1–5). The homozygous Foxp2 (R552H)-KI mice (P8–P10) along with the homozygous Foxp2-KO mice showed severe motor abnormalities, such as decreased spontaneous activity and sudden irregular and discoordinated movements. They were nearly unable to perform activities during P14–P20, while most heterozygous Foxp2 (R552H)-KI mice appeared to show normal activity, except for a small percentage of the population (<2%) showing severe reduced weight and lack of activity, similar to homozygous Foxp2 (R552H)-KI mice. To further analyze the phenotype of the Foxp2 (R552H)-KI mice (P10), we carried out standard behavioral analyses of three littermates (13 wild types, 20 heterozygotes, and five homozygotes), such as assessing righting reflex (Fig. 2*A*) and midair righting (Fig. 2*B*).

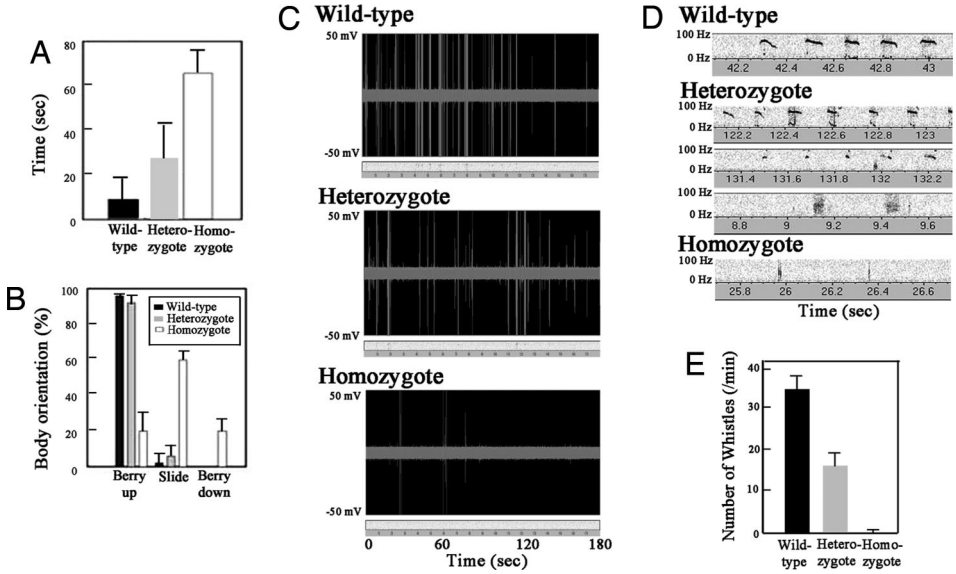

Fig. 2. Behavior analysis and USVs of the Foxp2 (R552H)-KI mice. (*A* and *B*) Righting reflex (*A*) and mid-air righting (*B*) of the Foxp2 wild-type and mutant mice. (*C*) Real-time spectrography of the USVs of pups (P8) after separation from the dam. (*D*) Major vocalization patterns (P8). Wild-type vocalization was mainly whistle-type USVs, whereas heterozygous Foxp2 (R552H)-KI mice produced three major vocalization patterns including USVs similar to the wild type (*Top*), short-length USVs (*Middle*), and click-type sonic vocalization (*Bottom*). Homozygous Foxp2 (R552H)-KI mice showed only a small number of click-type vocalizations. (*E*) Number of whistle-type USVs of pups (P8) per min. Vocalizations were recorded for 3–5 min.

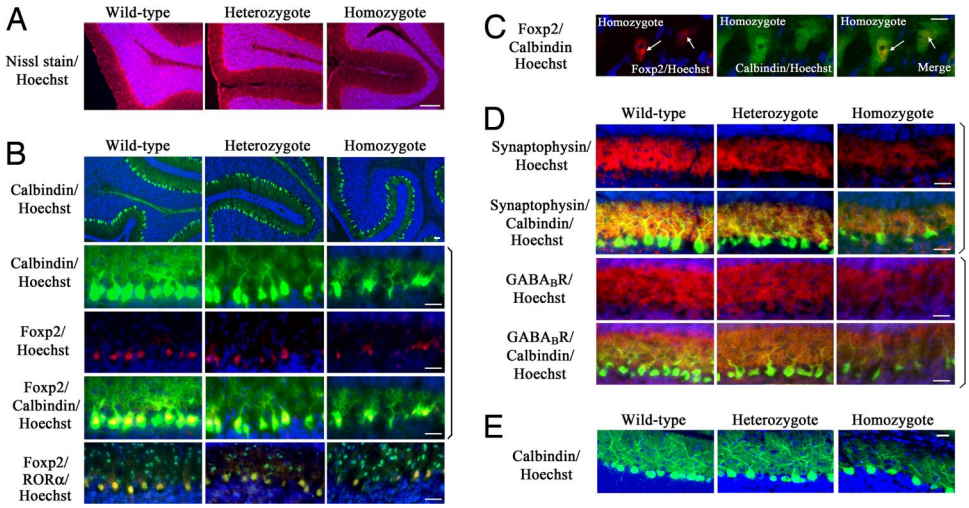

Fig. 3. Nuclear localization of Foxp2 (R552H) and its aggregates in the Purkinje cells and abnormal dendrites of Foxp2 (R552H)-KI mice. (*A*) Abnormality of Purkinje cells in the Foxp2 (R552H)-KI mouse. Nissl staining of the cerebellum (P19) (red) is shown. Nuclei of the granule cells are stained with Hoechst (blue). (*B*) Nuclear localization of Foxp2 (R552H) in the heterozygous and homozygous Purkinje cells (P10) and their immature dendrites. Calbindin and RORα are green, Foxp2 and Foxp2 (R552H) are red, and Hoechst is blue. (*C*) Nuclear aggregation of Foxp2 (R552H) in the homozygous Purkinje cells (P10). Arrows indicate the nuclear aggregates of Foxp2 (R552H). (*D*) Synapses in the immature dendrites of the homozygous and heterozygous Purkinje cells (P10). Calbindin is green, synaptophysin and GABABR are red, and Hoechst is blue. (*E*) Calbindin immunoreactivities of Purkinje cells of P19. Homozygous Purkinje cells showed immature dendrites, whereas heterozygous ones showed the mature dendrites like wild-type ones. Calbindin is green, and Hoechst is blue. (Scale bars: *A*, 1 mm; *B*, *D*, and *E*, 25 μm; *C*, 10 μm.) To eliminate variations due to regional differences, the descriptions that follow are based on sections taken from the same regions (folia III–V) in the central part of the cerebellum of the wild, heterozygous, and homozygous Foxp2 (R552H) mice.

Homozygous Foxp2 (R552H)-KI pups were delayed in their ability to right themselves when placed on their backs or in midair, whereas most heterozygous Foxp2 (R552H) mice did not exhibit obvious delays; the righting reflex of homozygous and heterozygous mice was seven and three times more delayed than wild-type mice, respectively (Fig. 2*A*). Furthermore, homozygous mice showed a clear difference from wild-type mice in the midair-righting assay, but heterozygous mice were not significantly different from wild type (Fig. 2*B*).

When isolated from the mother and littermates, infant rodents emit USVs, whistle-like sounds with frequencies between 40 and 100 kHz, as an important communicative signal in mother–offspring interactions (15). We assessed the number of USVs (whistles) and sonic/USVs (clicks) of 8-day-old pups after separation from the mother (Fig. 2*C*). Wild-type pups mainly produced whistle-type USVs, whereas heterozygous Foxp2 (R552H)-KI pups showed modest impairment for USVs; they produced three major vocalizations, including USVs similar to the wild type, short-length USVs, and click-type sonic vocalizations (Fig. 2 *D* and *E*). In addition, the mean number of USVs was reduced (Fig. 2*E*). Homozygous Foxp2 (R552H)-KI pups as well as homozygous Foxp2-KO pups showed severe impairment in the number of USVs (Fig. 2 *C* and *E*), and several pups produced only a few click-like vocalizations (Fig. 2*D*). Homozygous Foxp2 (R552H)-KI mice (P14–P20) did not produce any USVs because of a severe loss or near cessation of activity (unpublished observations).

Histochemical Alteration of the Brain of Foxp2 (R552H)-KI Mice. ***Cerebellum.*** In the cerebellum of the homozygous and heterozygous Foxp2 (R552H)-KI mice (P19), granule cells migrated normally from the external granule layer into the internal granule layer (Fig. 3*A*). The calbindin-positive Purkinje cells were aligned in a continuous row but were sparsely localized in the folia (P10). Foxp2 (R552H) and Foxp2 were expressed in the calbindin-positive Purkinje cells in the cerebellum (Fig. 3*B*). In contrast with *in vitro* studies (8, 9), Foxp2 (R552H) localized in the nuclei of Purkinje cells from homozygous Foxp2 (R552H)-KI mice, as did Foxp2 in the wild-type cells, and colocalized with nuclear receptor RORα (retinoic acid receptor-related orphan receptor-α) (17) (Fig. 3*B*). No Foxp2 was detected in RORα-positive basket cells and stellate cells. Foxp2 (R552H) showed nuclear aggregation in some of the Purkinje cells of homozygous Foxp2 (R552H)-KI mice (Fig. 3*C*).

The dendritic shafts of the homozygous Purkinje cells were thin, with less elaborated calbindin-positive dendritic arbors and reduced synaptophysin reactivity, a marker of synapse, compared with the wild-type Purkinje cells (Fig. 3*D*). Synaptophysin reactivity in the dendritic arbors of the heterozygous cells was at a level between that in the homozygote and the wild type (Fig. 3*D*). In the developing cerebellum of the wild type (P10), the metabotropic GABA receptor (GABABR) was strongly expressed in the dendrites of Purkinje cells, where the parallel fibers synapse (18), and in the migrating granule cells located just below the external granule layer (Fig. 3*D*). In the homozygous and heterozygous Foxp2 (R552H)-KI mice, GABABR was more poorly expressed in the dendrites although it was expressed in the migrating granule cells. At P19 and P45 the heterozygous dendrites had recovered and elaborated as well as wild-type dendrites (Fig. 3 *E* and SI Fig. 7), but the homozygous dendrites still remained at an immature level at P19 (Fig. 3*E*).

Cerebrum. In the wild-type mice, anti-Foxp2 reactivity was detected in the nuclei of the cortical plate, basal ganglia, striatum, and thalamus and weakly in the hippocampus in the cerebrum (Fig. 4*A*) (13, 14). Stronger anti-Foxp2 staining was observed in the CA1 hippocampus, thalamus, and striatum of the homozygous Foxp2 (R552H)-KI mice than in the wild type compared with anti-NeuN staining (Fig. 4 *A–I*). In the homozygous and heterozygous Foxp2 (R552H)-KI mice, Foxp2 and Foxp2 (R552H) were clearly detected in CA1 hippocampus neurons, but CA3 and the dentate gyrus were negative for anti-Foxp2 reactivity (Fig. 4 *D–F*). Furthermore, in the cortical plates, thalamus, striatum, hippocampus, and inferior olive, the Foxp2 (R552H)-KI neurons exhibited aggregates in the larger foci with strong anti-Foxp2 intensity in interphase nuclei, compared with the nuclei of the wild-type neurons, which exhibited small foci with a punctate nuclear staining pattern (Fig. 4 *J–L*).

Foxp2 (R552H) Aggregation and Stress. Cytoplasmic polyQ aggregates induce endoplasmic reticulum (ER) stress in cells (19). In

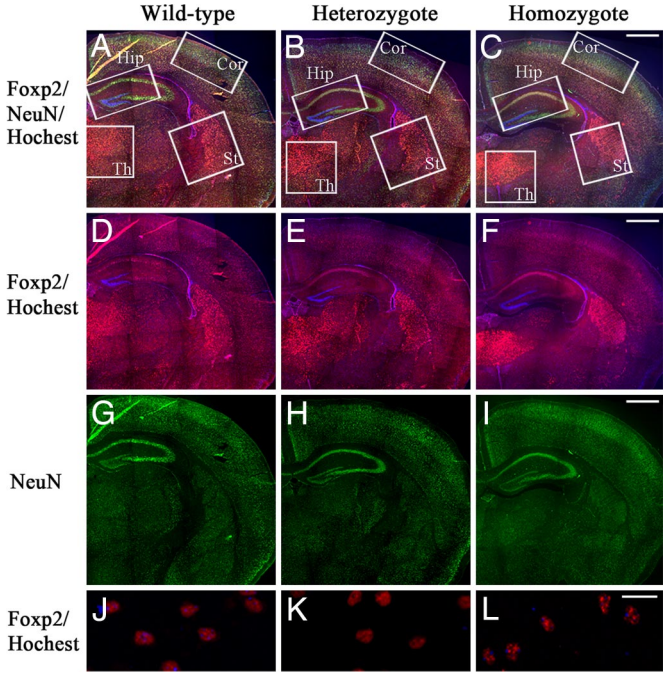

Fig. 4. Nuclear localization of Foxp2 (R552H) and its aggregates in the cerebral neurons. (*A–I*) Distribution of Foxp2 and Foxp2 (R552H) in the cerebrum of the 10-day-old wild type (*A*, *D*, and *G*), heterozygotes (*B*, *E*, and *H*), and homozygotes (*C*, *F*, and *I*). (*A–C*) Merged pictures with anti-NeuN (green), anti-Foxp2 (red), and Hoechst (blue). (*D–F*) Merged pictures with anti-Foxp2 and Hoechst. (*G–I*) Anti-NeuN. (*J–L*) Nuclear aggregation of Foxp2 (R552H) in the cortex neurons. (*J*) Wild type. (*K*) Heterozygote. (*L*) Homozygote. St, striatum; Th, thalamus; Cor, cortex; Hip, hippocampus. (Scale bars: *A–I*, 500 μm; *J–L*, 25 μm.)

contrast with the results of the brains of homozygous Foxp2 (R552H)-KI mice, ectopically expressed Foxp2 (R552H) localized in the cytoplasm and nuclei of C2C5 cells and COS cells (9) and aggregated in the cytoplasm and nuclei in a time-dependent manner by 24 h. Cells expressing Foxp2 (R552H) aggregates showed increased c-Jun phosphorylation (c-Jun-p) (Fig. 5*E*), increased eIF2α-phosphorylation (eIF2α-p) (Fig. 5*F*), up-regulation of CHOP (Fig. 5*G*), and activation of caspase-12 (anti-m12D341 reactivity) (Fig. 5*H*), all markers of ER stress. Notably, cells expressing Foxp2 were negative for each of these markers (Fig. 5 *A–D*). Thus, cytoplasmic and/or nuclear aggregates of ectopically expressed Foxp2 (R552H) induced the ER stress in cells. However,

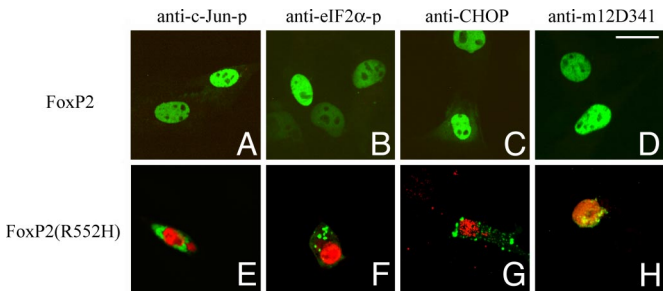

Fig. 5. Foxp2 (R552H) aggregates and ER stress. C2C5 cells were transfected with pEGFP-Foxp2 and Foxp2 (R552H). GFP-Foxp2 (R552H) showed cytoplasmic and nuclear aggregates in 24 h, whereas GFP-Foxp2 was located in the nuclei and showed no aggregation. Shown are Foxp2 (*A–D*) and Foxp2 (R552H) (*E–H*) (green). (*A* and *E*) Anti-c-Jun-p. (*B* and *F*) Anti-eIF2α-p. (*C* and *G*) Anti-CHOP. (*D* and *H*) Anti-m12D341 (antiactivated caspase-12) (red). (Scale bar: 25 μm.)

we could not detect any stimulation of ER stress and apoptotic signals in the Purkinje cells and cerebral neurons expressing Foxp2 (R552H) from the homozygous and heterozygous Foxp2 (R552H)-KI brains (P10) (unpublished observation).

Microarray Analysis. To identify potential candidate genes related to the Foxp2-mediated USVs, we focused on up-regulated and down-regulated genes in both homozygous and heterozygous Foxp2 (R552H) cerebrum or cerebellum. Microarray analysis of the homozygous or heterozygous and wild-type brain (P8) revealed a panel of up-regulated and down-regulated genes in response to the Foxp2 (R552H) mutation (SI Table 1). Well known genes up-regulated in both the heterozygous and homozygous mouse included protachykinin 1 precursor (*Tac1*) and GABA receptor (*Gabra5*) in the cerebellum and *Gabra2* in the cerebrum, whereas *Nhlh1* and *G0/S2* were down-regulated in the cerebellum and cerebrum, respectively. Furthermore, G protein-coupled receptor 15-like (*Pgr15l*) was down-regulated in the homozygous cerebellum and cerebrum but not in the heterozygous samples.

Discussion

Common Molecular Mechanism Shared with Mouse USVs and Human Speech. Accumulating evidence suggests that Foxp2 plays a general role in communication in multiple species: the FOXP2 (R553H) mutation was found in the KE family with a speech-language disorder (1–3), the expression pattern of Foxp2 in humans, mice, and songbirds is quite similar (11, 13, 14), the distribution of Foxp2 changes in songbirds during vocal learning (11), and Foxp2-KO mice lacking Foxp2 show abnormal USVs (16). Thus, FoxP2 is essential for not only human speech-language activity but also the USV production of mice and vocalization of songbirds. However, whether human speech and mouse USVs share a common Foxp2-mediated molecular mechanism has not been clear. Foxp2 contains many multifunctional domains and exhibits various alternative splicing products (16). Unlike the affected KE members expressing the FOXP2 (R553H) mutant, Foxp2-KO mice may be completely deficient for all of the functions of Foxp2 and its alternative splicing products (16, 20). Which functional domain of Foxp2 or alternative splicing product of Foxp2 functions in the molecular mechanism of mouse USVs and whether the phenotype of Foxp2-KO mice is due to the loss of function of forkhead domain were not previously established. In the present study we demonstrated that the homozygous Foxp2 (R552H)-KI mouse with a mutation similar to R553H in the KE family also showed abnormal USVs. Thus, mouse USVs and human speech share a common molecular mechanism, which is regulated by the forkhead domain of Foxp2 but impaired by its point mutation.

In *in vitro* cell culture experiments, two possible factors have been proposed for the mutated FOXP2, FOXP2 (R553H)-induced and FOXP2 (R328X)-induced impairment of speech-language ability (8–10): one is the lack of DNA binding activity (8), and the other is mislocalization of mutated FOXP2 (8, 9). Foxp2 (R552H) and Foxp2 localized in the nuclei of the Purkinje cells and cerebral neurons (Figs. 3 and 4), supporting the former possibility; thus, it is likely that the impairment of human speech and impairment of mouse USV result from the abolishment of FOXP2 transcriptional activity. Mouse USVs and human speech share a common molecular mechanism regulated by Foxp2 transcriptional activity.

At present, however, the genes regulating USV function and the development of the cerebellum and the maturation of Purkinje cells are unknown. Microarray analysis suggested several well known genes as candidates for targets of Foxp2 regulation in the developing brain (SI Table 1). *G0/S2* is a gene involved in the G_0–G_1 transition that is up-regulated during differentiation upon treatment with retinoic acid (21, 22). *G0/S2* was down-regulated in the homozygous and heterozygous Foxp2 (R552H)-KI brain, suggesting the delay of the cerebral development in the homozygous and heterozygous Foxp2 (R552H)-KI brain. Down-regulation of *Nhlh1*,

which encodes a helix–loop–helix transcriptional protein involved in the differentiation of neural cells and cerebellar development (23), also suggests the immature development of the neuronal cells in the homozygous and heterozygous Foxp2 (R552H) cerebellum. At present, the biological significance of up-regulation of *Tac1* is not known, but it may be worth noting that *Tac1* is a precursor of substance P expressed in area X of songbirds' brains, in which Foxp2 is up-regulated during vocal learning (11). Furthermore, up-regulation of *Gabra* may be associated with language impairment in some autistic patients (24) because impairment of social behavior is accompanied by an increase in inhibitory synaptic transmission as recently shown in the neuroligin-3 (R451C) knockin mice, the model mouse for autism (25). *Pgr15l*, which is highly expressed in numerous subregions of the hypothalamus (26), was down-regulated in the homozygous Foxp2 (R552H) cerebrum and cerebellum.

Immature Cerebellar Development with Abnormal Dendrites and USVs and Motor Impairment. The cerebellum is involved in coordinated movement. The Foxp2 (R552H) mutation prevented the development of the cerebellum and the maturation of the dendrites of the Purkinje cells (Fig. 3*B*) but did not prevent the migration of granule cells from the external granule layer into the internal granule layer (Fig. 3*A*), suggesting that the maturation of Purkinje cells is closely associated with the development of the cerebellum. However, the heterozygous mice with normal morphological development of the cerebellum showed poorer dendrite arbors of Purkinje cells and less abundant synaptophysin than wild-type mice (Fig. 3 *B* and *D*), suggesting that the USV and motor impairment of the heterozygous and homozygous Foxp2 (R552H)-KI mice are closely associated with the immature dendritic array of Purkinje cells rather than with the immature development of the cerebellum including incomplete folia formation (Fig. 3). Thus, it is likely that the Foxp2 (R552H) mutation causes the immature development of Purkinje cells with poor dendrites, resulting in the reduction of the number of synapses on the parallel fibers causing the differences in the USVs and motor impairment.

The USVs and motor impairment in the homozygous Foxp2 (R552H)-KI and Foxp2-KO mice suggest that (*i*) Foxp2 is independently essential for the motor neural system and USV neural system or (*ii*) Foxp2 is essential for the neural system, which is shared with the motor and USV neural system. The affected members (heterozygotes) of the KE family have an impaired ability to perform coordinated movements that are required for speech, verbal dyspraxia, and orofacial impairment but do not show abnormalities in single simple oral movements and limb praxis. Some of the affected members of the KE family have problems not only with speech but also with complex non-speech mouth movement; these two abnormalities are not significantly correlated with each other in these individuals. Thus, speech impairment is not correlated with the impairment of general movement but instead the impairment of some special coordinated movement.

Heterozygous Foxp2 (R552H)-KI mice also showed slight motor impairment (Fig. 2 *A* and *B*), except for a small percentage of the population showing low motor activity, and impairment of USV quality such as short-length USVs (Fig. 2*D*), suggesting that a particular part of the motor system, but not the entire motor system, is shared with the USV neural system. In humans, two neural systems, the temporal lobe and frontal basal ganglia, parietal, and cerebellar structures, have been proposed to be involved in language (27), and the cerebro-thalamo-cortical neural system is involved in the motor neural system. The neural system shared with the motor neural and USV (speech) learning neural brain systems within the neurocognitive framework must be addressed by further anatomical, physiological, and biochemical analysis of the heterozygous Foxp2 (R552H)-KI mice. The heterozygous Foxp2 (R552H)-KI mouse model presented here will be a useful model system for the study of the molecular mechanism causing the USV (speech) impairment.

Nuclear Aggregates in the Purkinje Cells and Cerebral Neurons. Foxp2 has two NLS signals flanking both ends of the forkhead domain and translocates to the nuclei to form foci *in vitro* (9). Foxp2 (R552H) showed cytoplasmic and nuclear localization *in vitro* (Fig. 5) (9), whereas in the brain it predominantly showed nuclear localization in the neuronal cells. Foxp2 (R552H) aggregated in the cytoplasm and nucleus *in vitro* by 24 h, and also in the nucleus of the Purkinje cells (P10) (Fig. 3*C*). This suggests that R552 may not be essential for Foxp2 nuclear localization and that the R552H mutation may induce a conformational change causing self-aggregation, likely via the polyglutamine tract (40 mer). Cytoplasmic or nuclear aggregates of Foxp2 (R552H) may be due to the balance between the nuclear translocation system and the self-aggregation of Foxp2 (R552H). This balance may be cell type-dependent, and in the developing neurons nuclear translocation could be faster than self-aggregation of Foxp2 (R552H), resulting in nuclear aggregation rather than cytoplasmic aggregation. However, Foxp2-KO mice showed severe motor impairment as well as abnormal USVs (P10), suggesting that the nuclear aggregates are not directly involved in the USV and motor impairment (P10).

Foxp2 (R552H) nuclear and/or cytoplasmic aggregates caused ER stress *in vitro* in cell culture (Fig. 5 *E–H*), probably because of the polyglutamine region, because similar observations were detected in cells expressing polyQ cytoplasmic aggregates (19). However, in the homozygous Foxp2 (R552H) brain, apoptotic markers, such as TUNEL and antiactivated caspase-3, and ER stress markers, such as anti-Jun-P and CHOP up-regulation, were negative in Purkinje cells and the cerebral neurons expressing Foxp2 (R552H) (unpublished observations). In patients with Huntington's disease, apoptotic cell death has not been observed, but in the Huntington's R6/2 mouse model containing a polyQ tract (144 mer) (28), ER stress was detected (29). Thus, cell death and ER stress may not always be related to the mutated protein aggregates. The cell death may depend on the type of aggregates such as cytoplasmic or nuclear aggregates, cell types, and developmental stages. The nuclear aggregates of Foxp2 (R552H) with a polyQ tract (40 mer) may induce the cell death of Purkinje cells or cerebral neurons in the latter developmental stages, causing severe movement defects. Otherwise, Foxp2 (R552H) nuclear aggregates could potentially induce continuous weak stresses that may cause the dysfunction of the cerebral neural system and cerebellar motor neural system regulating the coordinated movements closely associated with USVs and the speech-language neural system. The Foxp2 (R552H) nuclear or Foxp2 (R327X) cytoplasmic aggregate-induced stress and USVs and motor impairment remain to be studied further.

Here we demonstrated that Foxp2 (R552H)-KI mice related to the speech-language disorder showed USV and motor impairment and immature Purkinje cells with poor dendrites and fewer synapses. Some of the neurons of homozygous Foxp2 (R552H) mice contained nuclear aggregates of Foxp2 (R552H). The Foxp2 (R552H)-KI mice will be useful for the analysis of the common molecular mechanism shared with mouse USV and human speech and the pathogenesis of speech-language disorders.

Materials and Methods

Knockin Construct. A targeting vector for introducing G-to-A transition into exon 17 of the mouse Foxp2 gene locus was constructed by bacterial artificial chromosome (BAC) recombineering using Red/ET recombination (Gene Bridges). The mouse Foxp2 BAC clone, RP22-156B15, was obtained from the BAC PI derived artificial chromosome (BACPAC) Resources Center at Children's Hospital Oakland Research Institute. To introduce the mutation, an *rpsL-neo* counter selection cassette was inserted into exon 17 of the Foxp2 gene and was subsequently replaced with the PCR-amplified G-to-A transition sequence. A floxed *neo* selection marker for ES cell selection was introduced into intron 17. The Foxp2 (R552H) knockin targeting vector was finally constructed into pBluescript-MCA/DTA plasmid by subcloning the 7.6 kb of upstream and 3.9 kb of downstream sequence of

the manipulated Foxp2 gene. The targeting plasmid was sequenced to confirm the G-to-A transition and floxed *neo* insertion.

Foxp2 (R552H)-KI Mice. Mouse ES cells (PhoenixBio) derived from a 129S6/SvEvTac mouse were used for gene targeting. ES cells were electroporated with the targeting vector, and G418-resistant clones were isolated. Targeted ES clones were screened by Southern blot hybridization with 3′ flanking probe. To remove the *PGK-neo* marker cassette, a correctly targeted ES cell clone was transfected with the *Cre* expression plasmid and grown in the absence of G418 as described (30). Loss of *neo* was determined by Southern blot hybridization with the internal KI probe. Mutant mice were generated by injection of correctly targeted ES cells into C57BL/6 blastocysts. F_1 mice were bred by crossing of chimeric male offspring and C57BL/6 female mice. Germ-line transmission of the mutant Foxp2 locus was assessed by Southern blot hybridization with the internal KI probe. To generate animals homozygous for the targeted mutation, heterozygous animals were intercrossed.

Histopathology. The mice were anesthetized and killed by intracardiac perfusion of 10% formalin. The brain was fixed and embedded in paraffin. Coronal sections for cerebral hemispheres and transverse sections for cerebellum with pons were cut at 6-μm thickness. The sections were stained with hematoxylin and eosin and with a Neurotrace 530/615 Nissl stain (Molecular Probes).

Genotype Assay by PCR. One loxP sequence (ATAACTTCGTATAGCATACATTAT-ACGAAGTTAT) still remained in the intron between exons 17 and 18 in the targeted alleles after Cre-mediated removal of the PGK-neo Marker cassette. To identify the wild-type and targeted alleles, we performed PCR using primer pairs 5′-GATGGTCAAGACCCACTAGT-3′ for forward primer and 5′-AGGAGGAGACAG-CATGCATT-3′ for reverse primer.

Behavior Test. Animals selected from three distinct littermates were tested in behavioral analyses. Behavior tests including righting and midair righting were carried out on P6–P10 after the vocalization test. The righting reflex was evaluated by turning the mouse onto its back and noting the delay before it could turn itself over. For the midair-righting test, the pups were dropped from 30 cm above a padded surface to observe whether they could right themselves before landing (16).

Vocalization. Animals were assessed for USV monitoring before behavioral testing on P8 and P10. Each pup was separated from its littermates, one at a time, and placed in a shallow beaker in a soundproof chamber. The pup was then positioned in the chamber below a microphone connected with the UltraSound Gate 116 detector set (Avisoft Bioacoustic) to detect USVs at 40–100 kHz. Analysis started after the pup had been habituated to the chamber for 60 seconds; sounds were recorded for 3–5 min and then saved for later analysis.

Microarray Analysis. Total RNA of the cerebrum and cerebellum was isolated and purified from mice (P8) by using the RNeasy Mini kit (Qiagen). Fluorescent first-strand cDNA was prepared by reverse transcription (SuperScript II; Invitrogen) using primers 5′-labeled with Cy-dyes (Cy5). OpArrays slides (Operon), which printed the global 70-mer oligonucleotide array probes covering ≈25,000 genes and 38,000 transcripts, were used for microarray analysis. Slides were scanned on a Molecular Dynamics Generation III scanner to detect Cy5 fluorescence. Raw data analysis was carried out by using Array Vision 4.0 (Imaging Research).

Site-Directed Mutagenesis. To generate the Foxp2 (R552H) mutant, site-directed mutagenesis was performed by using the QuikChange II Site-Directed Mutagenesis kit (Stratagene) with the following primers: sense primer, 5′-AAGAATGCAG-TACATCATAATCTTAGC-3′; antisense primer, 5′-GCTAAGATTATGATGTACTG-CATTCTT-3′. Underlined nucleotides were mutated sites. Mutations were confirmed by DNA sequencing.

DNA Construction. The full Foxp2 cDNA was isolated from a mouse brain library (9). Primers for PCR amplification of Foxp2 cDNA were as follows: full length of Foxp2 using the forward primer 5′-ATGATGCAGGAATCTGCGACAG-3′ and the reverse primer 5′-TCATTCCAGGTCCTCAGATAAAGGC-3′. The PCR product was cloned into the pGEM-T easy vector (Promega) and then subcloned in-frame into the EcoR1 site of the pEGFP-C1 expression vector (Clontech).

Cell Culture and Transfection. C2C5 Cells were cultured at 37°C in a humidified atmosphere containing 5% CO_2 using α-MEM (Sigma) containing 10% FBS. Transfection was performed by using Lipofectamine 2000 (Invitrogen) according to the manufacturer's instructions.

Immunostaining. Wild-type and Foxp2 (R552H)-KI brains were fixed in 4% paraformaldehyde in PBS at 4°C overnight. Frozen sections (10 μm thick) were cut on a cryostat and immunostained with rabbit anti-Foxp2 (Abcam), rabbit anti-$GABA_BR$ (Alomone), rabbit and mouse anti-calbindin (Sigma), mouse anti-NeuN (Millipore), mouse anti-synaptophysin (Chemicon), or goat anti-RORα (Santa Cruz Biotechnology). For the immunostaining for the C2C5 cells, the transfected cells were fixed in 4% paraformaldehyde, washed with PBS, and then incubated with rabbit anti-c-Jun-p and anti-eIF2α-p (Cell Signaling Technology), mouse anti-CHOP (Santa Cruz Biotechnology), and rabbit anti-m12D341 (antiactivated caspase-12) (19) overnight at 4°C. Alexa Fluor 488- and Alexa Fluor 568-conjugated secondary antibodies against mouse, rabbit, and goat IgG were purchased from Molecular Probes. Nuclei were detected by Hoechst 33342 (Molecular Probes). The reactivity was viewed by using a confocal laser-scanning microscope (CSU-10; Yokogawa).

ACKNOWLEDGMENTS. We thank Dr. Shigeki Yuasa for valuable discussion during the study. This work was supported in part by Grants-in-Aid for Scientific Research on Priority Areas 18700333 and 19500305 from the Ministry of Education, Science, Sports, and Health Science Research from the Ministry of Health and Welfare of Japan, the Human Science Foundation.

1. Fisher SE, Vargha-Khadem F, Watkins KE, Monaco AP, Pembrey ME (1998) Localisation of a gene implicated in a severe speech and language disorder. *Nat Genet* 18:168–170.
2. Lai CS, Fisher SE, Hurst JA, Vargha-Khadem F, Monaco AP (2001) A forkhead-domain gene is mutated in a severe speech and language disorder. *Nature* 413:519–523.
3. Vargha-Khadem F, Gadian DG, Copp A, Mishkin M (2005) FOXP2 and the neuroanatomy of speech and language. *Nat Rev Neurosci* 6:131–138.
4. Marcus GF, Fisher SE (2003) FOXP2 in focus: What can genes tell us about speech and language? *Trends Cognit Sci* 7:257–262.
5. Liegeois F, *et al.* (2003) Language fMRI abnormalities associated with FOXP2 gene mutation. *Nat Neurosci* 6:1230–1237.
6. Shu W, Yang H, Zhang L, Lu MM, Morrisey EE (2001) Characterization of a new subfamily of winged-helix/forkhead (Fox) genes that are expressed in the lung and act as transcriptional repressors. *J Biol Chem* 276:27488–27397.
7. Li S, Weidenfeld J, Morrisey EE (2004) Transcriptional and DNA binding activity of the Foxp1/2/4 family is modulated by heterotypic and homotypic protein interactions. *Mol Cell Biol* 24:809–822.
8. Vernes SC, *et al.* (2006) Functional genetic analysis of mutations implicated in a human speech and language disorder. *Hum Mol Genet* 15:3154–3167.
9. Mizutani A, *et al.* (2007) Intracellular distribution of a speech/language disorder associated FOXP2 mutant. *Biochem Biophys Res Commun* 353:869–874.
10. Macdermot KD, *et al.* (2005) Identification of FOXP2 truncation as a novel cause of developmental speech and language deficits. *Am J Hum Genet* 76:1074–1080.
11. Haesler S, *et al.* (2004) FoxP2 expression in avian vocal learners and non-learners. *J Neurosci* 24:3164–3175.
12. Enard W, *et al.* (2002) Molecular evolution of FOXP2, a gene involved in speech and language. *Nature* 418:869–872.
13. Lai CS, Gerrelli D, Monaco AP, Fisher SE, Copp AJ (2003) FOXP2 expression during brain development coincides with adult sites of pathology in a severe speech and language disorder. *Brain* 126:2455–2462.
14. Takahashi K, Liu FC, Hirokawa K, Takahashi H (2003) Expression of Foxp2, a gene involved in speech and language, in the developing and adult striatum. *J Neurosci Res* 73:61–72.
15. Branchi I, Santucci D, Alleva E (2001) Ultrasonic vocalisation emitted by infant rodents: A tool for assessment of neurobehavioural development. *Behav Brain Res* 125:49–56.
16. Shu W, *et al.* (2005) Altered ultrasonic vocalization in mice with a disruption in the Foxp2 gene. *Proc Natl Acad Sci USA* 102:9643–9648.
17. Ino H (2004) Immunohistochemical characterization of the orphan nuclear receptor ROR alpha in the mouse nervous system. *J Histochem Cytochem* 52:311–323.
18. Lujan R, Shigemoto R (2006) Localization of metabotropic GABA receptor subunits GABAB1 and GABAB2 relative to synaptic sites in the rat developing cerebellum. *Eur J Neurosci* 23:1479–1490.
19. Kouroku Y, *et al.* (2002) Polyglutamine aggregates stimulate ER stress signals and caspase-12 activation. *Hum Mol Genet* 11:1505–1515.
20. Bruce HA, Margolis RL (2002) FOXP2: Novel exons, splice variants, and CAG repeat length stability. *Hum Genet* 111:136–144.
21. Ma Y, *et al.* (2003) Microarray analysis uncovers retinoid targets in human bronchial epithelial cells. *Oncogene* 22:4924–4932.
22. Zandbergen F, *et al.* (2005) The G0/G1 switch gene 2 is a novel PPAR target gene. *Biochem J* 392:313–324.
23. Duncan MK, Bordas L, Dicicco-Bloom E, Chada KK (1997) Expression of the helix-loop-helix genes Id-1 and NSCL-1 during cerebellar development. *Dev Dyn* 208:107–114.
24. Li H, Yamagata T, Mori M, Momoi MY (2005) Absence of causative mutations and presence of autism-related allele in FOXP2 in Japanese autistic patients. *Brain Dev* 27:207–210.
25. Tabuchi K, *et al.* (2007) A neuroligin-3 mutation implicated in autism increases inhibitory synaptic transmission in mice. *Science* 318:71–76.
26. Vassilatis DK, *et al.* (2003) The G protein-coupled receptor repertoires of human and mouse. *Proc Natl Acad Sci USA* 100:4903–4908.
27. Ullman MT (2001) A neurocognitive perspective on language: The declarative/procedural model. *Nat Rev Neurosci* 2:717–726.
28. Mangiarini L, *et al.* (1996) Exon 1 of the HD gene with an expanded CAG repeat is sufficient to cause a progressive neurological phenotype in transgenic mice. *Cell* 87:493–506.
29. Kouroku Y, *et al.* (2007) ER stress (PERK/eIF2alpha phosphorylation) mediates the polyglutamine-induced LC3 conversion, an essential step for autophagy formation. *Cell Death Differ* 14:230–239.
30. Muyrers JP, *et al.* (2000) Point mutation of bacterial artificial chromosomes by ET recombination. *EMBO Rep* 1:239–243.